Towards the development of poly(phenylene sulphide) based nanocomposites with enhanced mechanical, electrical and tribological properties

Ana M. Díez-Pascual, Mohammed Naffakh

GRAPHICAL ABSTRACT

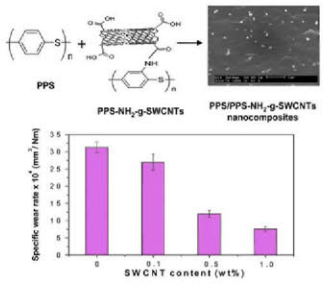

ABSTRACT

Novel poly(phenylene sulphide) (PPS) nanocomposites reinforced with an aminated derivative (PPS-NH_2) covalently attached to acid-treated single-walled carbon nanotubes (SWCNTs) were prepared via simple melt-blending technique. Their morphology, viscoelastic behaviour, electrical conductivity, mechanical and tribological properties were investigated. Scanning electron microscopy revealed that the grafting process was effective in uniformly dispersing the SWCNTs within the matrix. The storage and loss moduli as a function of frequency increased with the SWCNT content, tending to a plateau in the low-frequency regime. The electrical conductivity of the nanocomposites was considerably enhanced in the range 0.1–0.5 wt% SWCNTs; electrical and rheological percolation thresholds occurred at similar nanotube concentrations. Mechanical tests demonstrated that with only 1.0 wt% SWCNTs the Young's modulus and tensile strength of the matrix improved by 51 and 37%, respectively, without decrement in toughness, ascribed to a very efficient load transfer. A moderate decrease in the friction coefficient and a 75% reduction in wear rate were found for the abovementioned nanotube loading, indicating that PPS-NH_2-g-SWCNTs are good tribological additives for thermoplastic polymers. Based on the promising results obtained in this work, it is expected that these nanofillers will be used to develop high-performance thermoplastic/CNT nanocomposites for structural applications.

1. Introduction

Over the last years, carbon nanotubes (CNTs) have attracted particular interest because of their exceptional physical properties (high modulus and electrical/thermal conductivity) combined with their small diameter and very low density, which suggests that they are the next generation of nanofillers for polymer reinforcement [1,2]. Although CNTs are currently produced in large-scale quantities, the development of high-performance polymer/CNT composites has been hindered by the difficulty of achieving a homogeneous dispersion within the matrix and a strong CNT-polymer interfacial adhesion in order to attain effective load transfer. Without proper dispersion, filler aggregates tend to act as defect sites that limit the mechanical enhancement. To overcome

these problems, a variety of methods have been developed, such as the incorporation of functional groups onto the CNT surface via chemical modification, which can be performed either through covalent or non-covalent approaches [3]. The non-covalent strategy consists in the physical adsorption and/or wrapping of polymers around the CNT surface. The graphitic sidewalls of the CNTs are not altered, and allow $\pi-\pi$ stacking interactions with the adsorbed polymer. The main advantage of this approach is that preserves the intrinsic properties of the CNTs; however, the polymer wrapping decreases the aspect ratio of the reinforcement, and the forces between the CNTs and the polymer are weak, thus the efficiency of the load transfer in the composites might be low [4]. The covalent strategy generally involves nanotubes bound to carboxylic groups in amidation or esterification reactions with amine or hydroxyl groups of polymers or organic molecules [5,6]. The chemical bonding (grafting) of polymer chains to defect sites of the CNT surface results in composites with improved nanofiller dispersion and interfacial adhesion between the two phases; therefore, the mechanical properties of these composites are superior to those containing pristine CNTs. In fact, an ideal approach is to functionalize the CNTs with the matrix of the composite. Several polymers have been used for this purpose, including poly(vinyl alcohol) (PVA) [7], polystyrene (PS) [8] and polypropylene (PP) [9].

Poly(phenylene sulphide) (PPS) is a high-performance thermoplastic composed of phenyl rings and sulphur atoms that possesses outstanding mechanical and thermal properties [10]. It also exhibits good chemical and oxidation resistance as well as dimensional stability, minimum water absorption, inherent non-flammability, anti-ageing and excellent friction properties [11]. The most important application areas are automobiles, aircrafts, rail-mounted vehicles and electronics [12]. To extend its structural applications, different fillers such as glass fibres [13], inorganic nanoparticles (e.g. IF-WS_2) [14,15], carbon nanofibers (CNFs) [16] and multi-walled carbon nanotubes (MWCNTs) [17,18] have been melt-blended with PPS matrix. It has been reported [17] that the mechanical properties of PPS/MWCNT composites improve only marginally at low nanofiller contents. An effective way to attain improved performance would be the formation of covalent linkages at the CNT–PPS interface; however, the insolubility of this polymer in common organic solvents [19] and its lack of terminal end groups make difficult its functionalization, hence the grafting to other molecules.

The main aim of this work is to investigate the effect of an aminated PPS derivative (PPS-NH_2) covalently grafted onto the surface of acid-functionalized SWCNTs (SWCNT-COOH) as filler in a PPS matrix. The nanocomposites (PPS/PPS-NH_2-g-SWCNT) were prepared by the simple and conventional melt-blending technique, and were characterized in terms of their mechanical, electrical, rheological and tribological properties, comparing the results with those obtained for a reference composite reinforced directly with the acid-treated SWCNTs. To the best of our knowledge, there is no previous study related to the influence of polymer-grafted fillers on the wear behaviour of thermoplastic composites.

2. Experimental

2.1. Materials

PPS (Fortron 0205B4) was kindly supplied by Ticona in powder form, with an average particle size of 20 μm, $d_{25\ °C} = 1.35$ g cm^{-3}, $T_g = 90$ °C, $T_m = 280$ °C. The polymer was dried at 100 °C for 14 h and stored in a dry environment before blending. The aminated derivative (PPS-NH_2) was synthesized from a nitrated PPS polymer using sodium dithionite ($Na_2S_2O_4$) as reduction agent [20]; its degree of functionalization (~16%), defined as moles of NH_2 groups per mole of monomer of PPS, was determined by elemental analysis. CVD SWCNTs were provided by Cheap Tubes Inc, USA ($d_{25\ °C} = 2.1$ g cm^{-3}, diameter: 1–2 nm, length: 5–30 μm, amorphous carbon content ≤ 3 wt%, purity > 90%, elemental analysis: C, 97.32; Cl, 0.21; Fe, 0.56; Ni, 1.88; S, 0.03). They were oxidized in HNO_3 6 M at 120 °C for 4 h and the excess of acid and amorphous carbon impurities were removed by centrifugation. The resulting solid (SWCNT-COOH) was vacuum dried in an oven at 60 °C; the functionalization degree of the SWCNTs, ~7.1%, was determined from TGA (see Supplementary Information, Fig. S1). Grafting of PPS-NH_2 (5.5 g) onto the SWCNT-COOH (0.5 g) was carried out via direct esterification by activation of the carboxylic acids with dicyclohexylcarbodiimide (DCC). The polymer was dissolved in dimethylformamide (DMF, 25 mL) and kept at 50 °C for 24 h under stirring, followed by addition of a solution of DCC (23.1 g) and 4-dimethylaminopyrydine (DMAP, 1.7 g) in DMF (100 mL). Separately, SWCNT-COOH was also dispersed in DMF (10 mL) by ultrasonication. Subsequently, the polymer solution and nanotube dispersion were mixed and maintained for 20 h at 40 °C under argon flow and stirring. The grafted material (PPS-NH_2-g-SWCNT) was filtered, washed with methanol and dried under vacuum at 50 °C. The extent of the grafting reaction (38.7%) was calculated through the Kaiser test (see Supplementary Information). Taking into account the degree of functionalization of PPS-NH_2 [20], the amount of SWCNT-COOH and PPS-NH_2 used for the grafting process and the extent of this reaction, the average amount of PPS derivate grafted was estimated as ~6 mmol of monomers per gram of SWCNT.

2.2. Preparation of PPS based nanocomposites

The PPS/PPS-NH_2-g-SWCNT nanocomposites were prepared via melt-blending, after a pre-processing stage based on mechanical treatments in an organic solvent. Firstly, the PPS-NH_2-g-SWCNT was dispersed in a small volume of ethanol and mixed with the PPS powder. The mixture was then homogenized by mechanical stirring and bath ultrasonication for approximately 30 min, and subsequently dried in vacuum at 50 °C under a pressure of about 70 mbar until the ethanol was completely evaporated.

The melt-compounding of the resulting dispersions was performed with a Haake Rheocord 90 system operating at 320 °C, with a rotor speed of 150 rpm during 20 min. Three composites were prepared, with effective SWCNT contents of 0.1, 0.5 and 1.0 wt%, respectively. For comparative purposes, a nanocomposite reinforced with 1.0 wt% acid-treated SWCNTs was also prepared under the same processing conditions, and is designated by an asterisk (*). Prior to characterization, the composites were pressed as thin films in a hot-press system using two heating/cooling plates.

2.3. Scanning electron microscopy

The morphology and state of carbon nanotube dispersion within the matrix were evaluated with a Philips XL30 scanning electron microscope (SEM) applying an acceleration voltage of 25 kV and an intensity of $9 \cdot 10^{-9}$ A. Samples were cryo-fractured from film specimens and then were placed in a heated oven for 2 h at 180 °C in order to better identify the SWCNTs. The fractured samples were coated with a ~5 nm Au/Pd overlayer to avoid charging during electron irradiation.

2.4. Dynamic mechanical analysis

The dynamic mechanical performance of the composites was investigated using a Mettler DMA 861 dynamic mechanical analyser. Experiments were performed in the tensile mode, in the

temperature range between −100 and 250 °C, at a frequency of 1 Hz and heating rate of 2 °C min^{-1}. Measurements as a function of frequency were carried out in the range 10^{-2}–10^{3} Hz, at a temperature of 250 °C and 0.5% strain.

2.5. Tensile and flexural tests

Tensile and flexural properties were measured with an INSTRON 4204 mechanical tester at room temperature and 50 ± 5% relative humidity, using a crosshead speed of 1 mm min^{-1} and a load cell of 1 kN. Tensile specimens (Type V) and rectangular flexural coupons were employed, according to UNE-EN ISO 527-1 and 178 standards, respectively. All the samples were conditioned for 24 h before the measurements. The data reported are the average of the results for 5 specimens.

2.6. Charpy impact tests

Charpy notched impact strength measurements were carried out using a CEAST Fractovis dart impact tester. A hammer mass of 1.096 kg impacted at a constant velocity of 3.60 m s^{-1} (giving a total kinetic energy at impact of 7.10 J) on notched specimen bars with a V-shape notch tip radius = 0.25 mm, as described in the UNE-EN ISO 179 standard. Measurements were performed at 23 ± 2 °C and 50 ± 5% relative humidity. The presented data correspond to the average value of at least 6 specimens.

2.7. Tribological properties

Pin-on-disk tests were performed on a Microtest MT 400-98 apparatus, using a 6 mm diameter 100Cr6 steel ball like pattern slide. Measurements were carried out under a constant load of 5 N at a rotation speed of 375 rpm. The equipment was placed in an isolated box to control the atmosphere conditions, and the experiments were performed under air with a relative humidity of 22 ± 2% and temperature of 24 ± 2 °C. The wear experienced by the flat substrate was determined through the measurement of the wear-track profile by using a profilometer with a resolution of ~10 nm. Each tribological test was repeated three times to ensure reproducibility.

2.8. Surface energy determination

Contact angle measurements were carried out at room temperature on a Krüss G10 contact angle measurement system using the sessile drop method. Two liquids with different polarity (water and diiodomethane) were used to make the drops. The angles were measured by dropping with a syringe ten droplets (~0.5 μl) of each liquid on different positions of the solid surface. The image of the drop was captured by a video camera connected to a computer, and the analysis of the drop profile provided the contact angle value. Subsequently, the total surface energy and its polar and dispersion components were determined through the Owens–Wendt–Rabel–Kaelble equation [21]:

$$(1+\cos\theta)\sigma_l = 2\left(\sigma_s^d\sigma_l^d\right)^{1/2} + 2\left(\sigma_s^p\sigma_l^p\right)^{1/2} \quad (1)$$

where θ is the measured contact angle, σ_l is the total surface energy of the liquid in contact with the solid, σ_l^d, σ_l^p and σ_s^d, σ_s^p are the dispersion and polar components of the liquid and solid, respectively. For the calculations, literature data [20] of the surface energies of both liquids were used (water: $\sigma_l^p = 51.0$ mN/m, $\sigma_l^d = 21.8$ mN/m; diiodomethane: $\sigma_l^p = 2.3$ mN/m^{-1}, $\sigma_l^d = 48.5$ mN/m^{-1}).

2.9. Electrical conductivity measurements

Room temperature DC volume conductivity measurements were carried out on rectangular thin film samples using a four-point probe (FPP) device (Scientific Equipment, India) with a spacing probe $S = 0.2$ cm. A constant current I was applied to the bar specimen through two outside probes with the aid of a DC power supply (Model CCS-01) and the steady voltage V across the inside probes was measured with a digital microvoltmeter (Model DMV-001). The resistivity ρ was calculated through the equation:

$$\rho = (\pi/\ln 2)t(V/I)f_1f_2 \quad (2)$$

where t is the thickness of the sample, f_1 and f_2 are geometric correction factors. The volume conductivity $\sigma = \rho^{-1}$ was obtained assuming that $f_1 = 1$ for $t << S$, and taking $f_2 = 0.76$ for the rectangular geometry of the specimens used. 6 bars for each nanocomposite were tested to report an average value.

3. Results and discussion

3.1. Morphology and dispersion of the SWCNTs in the PPS matrix

Typical SEM micrographs from fractured specimens of PPS nanocomposites (1.0 wt% effective nanotube loading) prepared either by direct integration of the SWCNTs or via addition of the aminated derivative grafted to the nanotubes are compared in Fig. 1. The reference composite (Fig. 1a) displays poor SWCNT

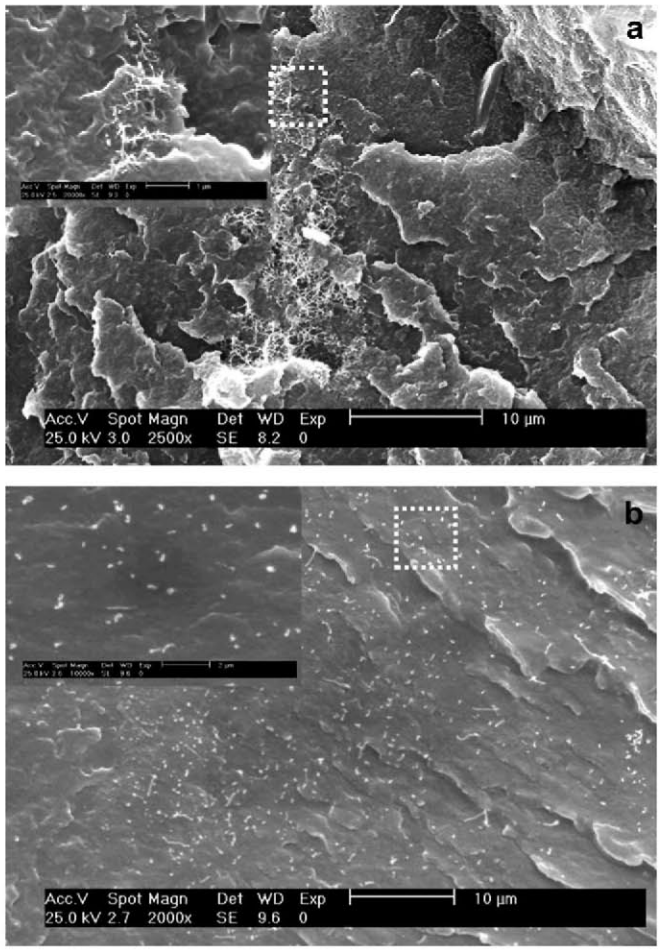

Fig. 1. SEM images from fractured surfaces of PPS nanocomposites with an effective CNT content of 1.0 wt%: (a) PPS/SWCNT*; (b) PPS/PPS-NH_2-g-SWCNT. The insets are higher magnification micrographs showing the filler phase.

dispersion, and micrometre-sized agglomerates can be observed. In contrast, the composite incorporating PPS-NH_2-g-SWCNTs (Fig. 1b) shows a very homogenous distribution of the nanotube bundles (which appear as bright spots) and a smoother surface topology. The average bundle diameter seems to be larger than that of the reference sample; this increase in size could be ascribed to the polymer coating around the nanotube surfaces. Similar behaviour of bundle diameter increment has been reported for poly(ether ketone)s grafted to MWCNTs [22]. The images reveal that the grafting process improved the dispersion of the SWCNTs, leading to larger nanofiller-matrix effective contact area.

3.2. Viscoelastic behaviour

The viscoelastic properties of the nanocomposites were evaluated, and the temperature dependence of the storage modulus (G') and tan δ at the frequency of 1 Hz are depicted in Fig. 2. For the sake of comparison, the curves of neat PPS and the aminated derivative are also included in the plot. As can be observed, the addition of SWCNTs leads to a noticeable improvement in the storage modulus of the matrix in the temperature range from −100 to 250 °C. Thus, G' of neat PPS at 25 °C is about 2 GPa, and increases by 17, 40 and 54% with the incorporation of 0.1, 0.5 and 1.0 wt% loading of SWCNTs anchored to PPS-NH_2. However, for the reference composite reinforced with 1.0 wt% SWCNTs, the increment was smaller (~26%). The significant stiffness enhancement attained in the nanocomposites prepared by polymer grafting should be related to the strong interfacial adhesion attained through the covalent bonding and the improved dispersion of the nanotubes within the matrix. In contrast, the agglomerates observed in the reference sample result in weak SWCNT-matrix adhesion, hence lead to less effective load transfer. These results are in agreement with the behaviour reported in previous works for the dynamic mechanical properties of different thermoplastic based nanocomposites such as PP [9], poly(ether ether ketone) (PEEK) [23] and poly(styrene-co-acrylonitrile) (SAN) [24], where the modulus of composites incorporating polymer-grafted CNTs were on average 50% higher than those reinforced directly with the CNTs.

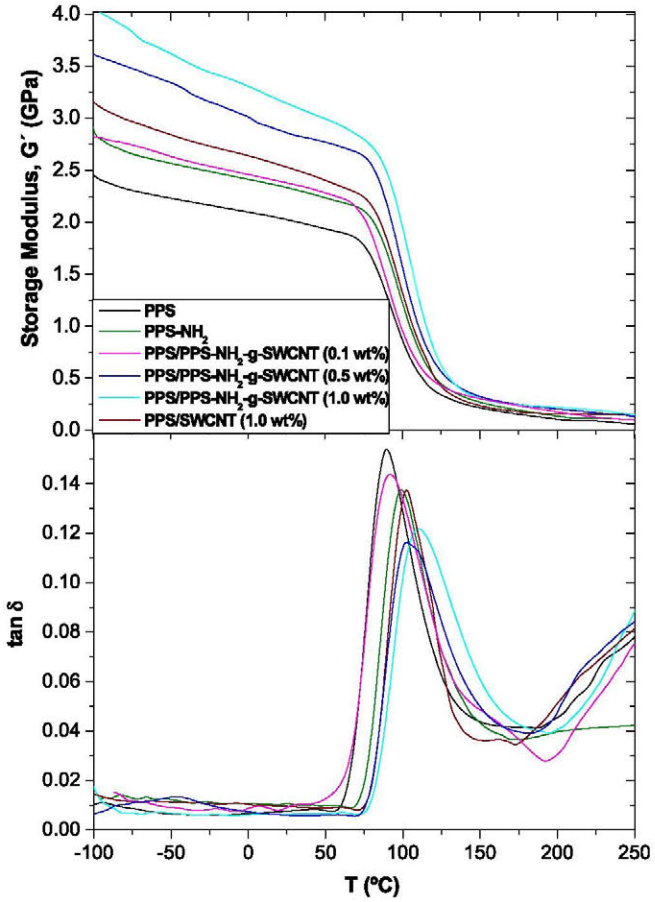

Fig. 2. Storage modulus G' and tan δ as a function of temperature, at a frequency of 1 Hz, for PPS, the aminated derivative and nanocomposites incorporating different SWCNT loadings.

The comparison of tan δ curves (ratio of the loss to storage modulus) as a function of temperature for neat PPS and the nanocomposites reveals a shift in the position of tan δ maximum (which corresponds to the glass transition temperature T_g) with increasing SWCNT content, the increment being around 20 °C for the composite with PPS-NH_2-g-SWCNTs (1.0 wt% effective loading). This suggests that polymer-grafted CNTs efficiently hamper the mobility of PPS chains, which is reflected in higher T_g values. Similar behaviour is found for the reference composite with 1.0 wt% acid-treated SWCNTs, although the increase was only 12 °C. The noticeable T_g increment observed in the composites incorporating PPS-NH_2 should be ascribed to the existence of strong interactions between the components through covalent and hydrogen bonds. Analogous behaviour of T_g enhancement has been reported for nanocomposites based on poly(ether ketone) matrices covalently anchored to CNTs [22,23]. However, other authors dealing with PS [8] and SAN [24] composites found a small decrease in the T_g with the addition of polymer-grafted MWCNTs, attributed to the lubricant role of the nanotube surface. It can also be observed from Fig. 2 that the height of tan δ peak decreases with the addition of these nanofillers, combined with a significant widening of the maximum. The reduction in height accounts for the SWCNT-matrix interactions, which increase as the nanofiller loading rises. This fall in tan δ_{max} value is more pronounced for nanocomposites incorporating PPS-NH_2-g-SWCNTs, indicating stronger filler-matrix interfacial adhesion. Furthermore, the aminated derivative also exhibits a diminution in the peak height in comparison to PPS, probably due to the large number of hydrogen bonds between adjacent chains. The broadening of tan δ peak can be related to the heterogeneous nature of the composites. The nanotubes perturb the relaxation of the polymer chains located in their vicinity, which would behave differently from those located in the bulk matrix, resulting in a wider maximum.

It is also interesting to analyse the influence of these nanofillers on the area under tan δ peak, which is indicative of the energy dissipated in the viscoelastic relaxations [25]. Experimentally, it is found that PPS-NH_2 shows around 7% smaller area than neat PPS, and the reference composite exhibits ~13% reduction. In the case of composites incorporating PPS-NH_2-g-SWCNTs, the area is about 8% higher than that of the pure matrix for 0.1 wt% loading, whilst it is approximately maintained for SWCNT contents of 0.5 and 1.0 wt %. These results indicate that the addition of a small amount of PPS-NH_2-g-SWCNTs increases the composite stiffness without detriment in its ability to dissipate energy. This behaviour differs from that commonly reported for thermoplastic/CNT composites [26], where a strong reduction in the area under tan δ peak was observed upon incorporation of the carbon nanotubes. This discrepancy can be explained considering that the addition of PPS-NH_2 leads to a more homogeneous SWCNT dispersion, hence less hindrance to the ductile flow of the matrix and lower stress concentration at the CNT–matrix interface. These synergic effects contribute to maintain the energy dissipation.

On the other hand, the addition of SWCNTs modifies the frequency dependence of the storage (G') and loss (G'') modulus at high temperatures (i.e. 250 °C, Fig. 3). As the nanotube content

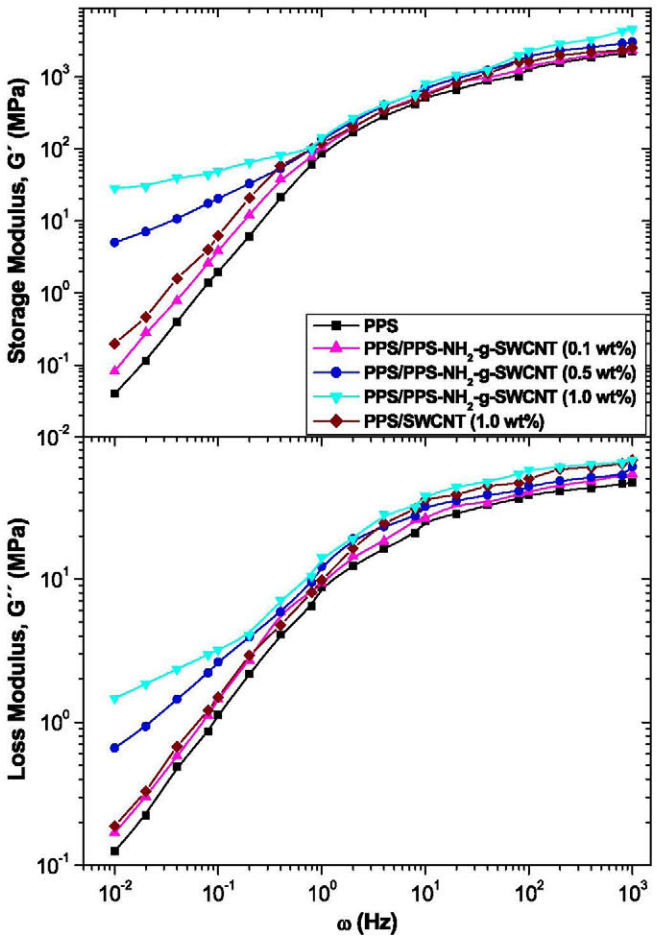

Fig. 3. Storage modulus and loss modulus as a function of frequency, at 250 °C, for neat PPS and nanocomposites with various SWCNT contents.

increases, the magnitude of both moduli rises, whilst the slope of the curves decreases. The differences between the composite moduli and those of the matrix are more pronounced at low frequencies. According to the theory of linear viscoelasticity [27], the storage and loss modulus of a homogeneous polymer in the low-frequency regime obey the following scaling law: $G' \sim \omega^2$ and $G'' \sim \omega$, indicating that the polymer chains are fully relaxed (terminal behaviour). However, in filler-reinforced polymer systems, they often deviate from the mentioned dependence, tending to a plateau like-regime, which indicates a transition from liquid-like to solid-like viscoelastic behaviour. The critical concentration at which this transition is observed is known as the rheological percolation threshold. Above this concentration, tube–tube interactions dominate over polymer–nanotube interactions, due to the formation of a network of CNTs. In PPS/PPS-NH_2-g-SWCNT composites, the low-frequency power-law dependence of G' decreases gradually with increasing nanotube content, the exponents being 1.70, 1.65, 0.69 and 0.52 for 0, 0.1, 0.5 and 1.0 wt% loadings, respectively. Similar trend is observed for G'', where the exponent decreases from 0.95 for neat PPS and the composite with 0.1 wt% content to 0.57 and 0.34 for those with 0.5 and 1.0 wt% loading. This non-terminal low-frequency behaviour observed for nanotube contents higher than 0.1 wt% is ascribed to the presence of a nanotube network, which restricts the long-range motion of the polymer chains. Similar viscoelastic behaviour has been reported for different thermoplastic nanocomposites containing CNTs [28,29]. At high frequencies, the nanotubes have only slight influence on the rheological behaviour, indicating that they hardly modify the short-range dynamics of PPS chains.

It has been reported [28] that the degree of nanotube dispersion strongly impacts the viscoelastic properties of polymer/CNT nanocomposites. Smaller low-frequency slopes of G' and G'' vs. frequency and higher moduli values are associated with enhanced nanotube dispersion. At low frequencies, the reference composite with 1.0 wt% SWCNTs shows almost the same slopes as neat PPS, and exhibits about one and two orders of magnitude lower G'' and G' values, respectively, than the composite incorporating PPS-NH_2-g-SWCNTs (1.0 wt% nanotube loading). This is consistent with the observations from SEM analysis, which revealed poorer nanofiller distribution for the composite prepared by direct integration of the SWCNTs. This reference sample has discrete nanotube-rich domains rather than a CNT network, hence the polymer chains flow independently of the nanotubes, and their motion should be very similar to those of neat PPS.

3.3. Electrical and rheological percolation behaviour

Fig. 4a shows the evolution of the storage modulus as a function of the nanotube loading at a fixed frequency of 10^{-2} Hz and 250 °C. A sudden change in the modulus appears in the range 0.25–0.30 wt

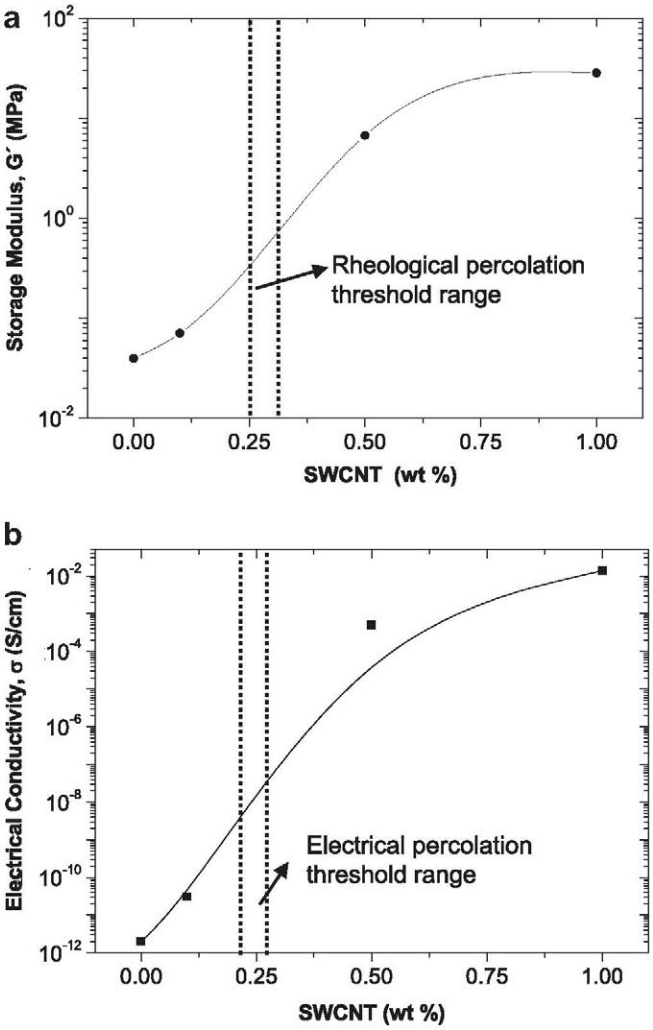

Fig. 4. Storage modulus at 250 °C and frequency of 10^{-2} Hz (a) and electrical conductivity (b) for PPS/PPS-NH_2-g-SWCNT nanocomposites as a function of the nanotube loading.

% SWCNTs, which corresponds to the rheological percolation threshold. At lower concentrations, the CNTs only restrict the local mobility of individual polymer chains. However, at the percolation threshold, these restrictions extend all over the composite, leading to the observed increase in G'. Generally, the formation of a CNT network affects both the rheological and electrical properties in a related manner [28]. To investigate the relationship between these properties, the electrical conductivity (σ) of PPS nanocomposites was measured, and the results are plotted in Fig. 4b. Neat PPS is an insulating polymer ($\sigma \sim 10^{-12}$ S cm^{-1} [30]), and its conductivity rises monotonously with increasing SWCNT content, showing typical percolation behaviour. At 0.1 wt% loading, the composite remains insulating ($\sigma < 10^{-8}$ S cm^{-1}); a sharp increment in σ of about eight orders of magnitude is observed in the range 0.1–0.5 wt% SWCNTs, whereas at higher loadings the conductivity rises only slightly. According to the experimental data, the critical concentration (Φ_C) at which electrically conductive networks of SWCNTs are formed lies around 0.25 wt%. Kovacs et al. [31] reported the existence of two electrical percolation thresholds in composites that possess a fluid state of low viscosity during processing. The higher is determined by the statistical percolation theory, which for a random distribution of CNTs with a typical aspect ratio of 1000 predicts a Φ_C of about 0.1 wt%. The lower is attributed to kinetic percolation, which allows for particle flocculation and network formation, appearing at lower concentrations. In these PPS based nanocomposites, the SWCNTs are very homogenously dispersed within the matrix, hence the Φ_C observed corresponds to a statistical percolation. Φ_C of CNT-filled thermoplastics such as polycarbonate (PC), PS and PP usually lies between 0.5 and 2.0 wt% [31]. Previous studies on PPS/MWCNT composites found Φ_C values of about 1.0 [32], 1.5 [17], and 5.0 wt% [18]. The critical concentration observed in this work is considerably lower than the reported results, which can be attributed to the enhanced filler dispersion, the stronger nanotube-matrix interfacial bonding and the higher aspect ratio of SWCNTs as compared to MWCNTs.

Regarding the influence of the polymer grafting on the composite conductivity, it is found that the reference sample exhibits a σ value of 2×10^{-3} S cm^{-1}, about one order of magnitude lower than that of the composite incorporating PPS-NH_2-g-SWCNTs (1.0 wt% loading). As known [1], polymer wrapping increases the tube–tube resistance, thereby leading to a reduction in conductivity. However, the covalent attachment of the aminated derivative onto the SWCNTs improved their dispersion, as revealed by SEM images; homogeneously dispersed CNTs possess higher aspect ratio than nanotube aggregates, resulting in higher conductivity. Previous studies have also reported similar [23] or even higher [33] σ values for composites with polymer-grafted CNTs as compared to those prepared by direct reinforcement.

It is worth mentioning that in this work the electrical and rheological percolation thresholds take place at similar SWCNT loadings. However, several studies [18,28,29] have reported that the electrical percolation occurs at higher concentration than the rheological, ascribed to the different tube–tube distances required to reach these phenomena. For electrical percolation, the distance should be small enough to allow electron hopping or tunnelling, whereas for rheological percolation it should be smaller than the radius of gyration of the polymer chains. Therefore, it might be that the average diameter of random coils of PPS chains is comparable to the inter-tube distance necessary for electrical percolation.

3.4. Mechanical properties

The static mechanical properties of the nanocomposites were investigated through tensile, flexural and Charpy impact tests. The average Young's modulus (E), tensile strength (σ_y), elongation at break (ε_b) and toughness (T) obtained from the tensile tests of the different samples at room temperature are displayed in Fig. 5. E of PPS is about 2.2 GPa, and increases moderately (~15%) for the aminated derivative (Fig. 5a). Regarding the nanocomposites, significant increments are found for those with covalent bonds,

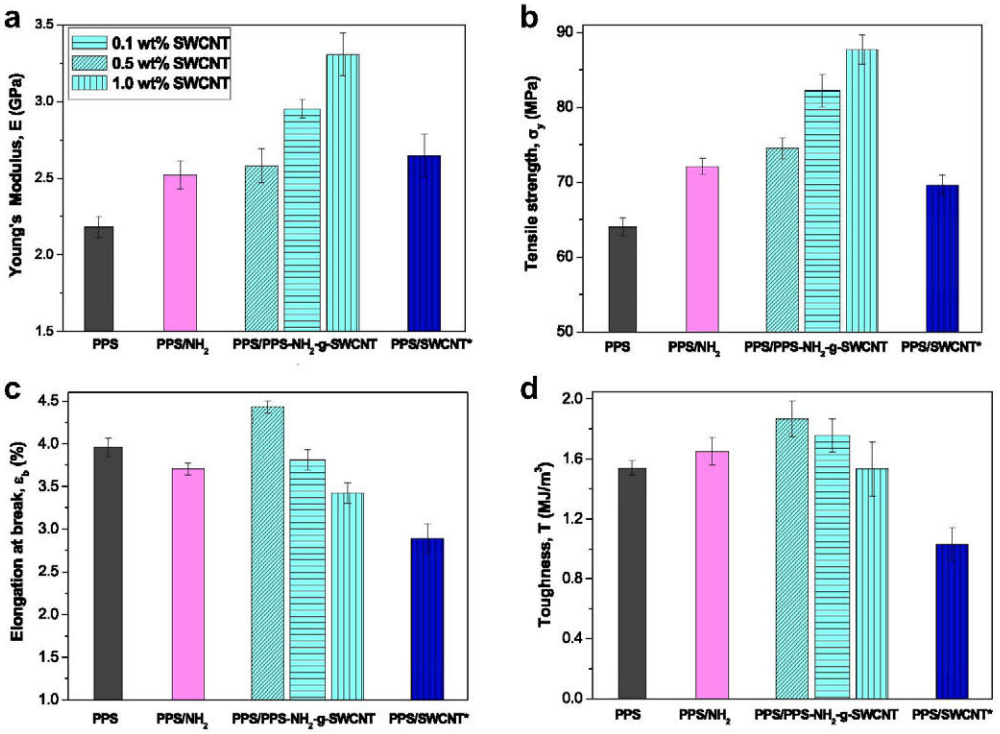

Fig. 5. Young's modulus E (a), tensile strength σ_y (b), elongation at break ε_b (c) and toughness T (d) for PPS/PPS-NH_2-g-SWCNT nanocomposites. For comparison, data of neat PPS, the reference composite PPS/SWCNT* and the aminated derivative PPS-NH2 are also plotted.

where E rises by ~17, 35 and 51% for effective loading fractions of 0.1, 0.5 and 1.0 wt%, respectively. In the case of the reference composite, the increment in modulus is less significant (~20%). The stronger increase in the composites with polymer-grafted fillers should arise from enhanced matrix-SWCNT load transfer, induced by more homogenous nanotube dispersion and stronger interfacial bonding between the components. Similar effects have been described for other thermoplastic composites incorporating polymer-grafted CNTs [9,23,24].

The experimental data obtained have been compared with the predictions of theoretical models such as the Krenchel's rule of mixtures for discontinuous reinforcement, which can be expressed as:

$$E_c = \left(\eta E_f - E_m\right)V_f + E_m \quad (3)$$

where E_f and E_m are the Young's modulus of the filler and matrix, respectively, V_f is the filler volume fraction and η the strengthening efficiency coefficient, which is assumed to be 1/5 for randomly oriented fillers [34]. Taking into account average reported values for the SWCNT modulus [35], experimental data of composites containing PPS-NH_2-g-SWCNTs exceed slightly the theoretical calculations in the concentration range studied; the differences are more pronounced at very low SWCNT loadings (i.e. 12% at 0.1 wt%) and become smaller at higher concentrations (i.e. 3% at 1.0 wt%). This might be explained considering that the nanotubes could be more curved at higher concentrations, due to stronger interactions with their neighbours, and the nanotube waviness decreases the reinforcing efficiency. On the other hand, the experimental value of the reference composite falls considerably below the theoretical predictions (about 18% difference). This is attributed to the presence of small aggregates, whilst the model assumes individually dispersed nanotubes. Other studies dealing with polymer-grafted CNT composites found results in good agreement [8,9] or even higher [23,24] than the theoretical calculations up to 1% loading, whereas for composites prepared by direct reinforcement, the experimental data were remarkably lower than the predictions for concentrations above 0.01% [8,23].

The tensile strength σ_y (Fig. 5b) displays similar trends to those described for the modulus, the increments being more pronounced at low SWCNT contents. The composite with PPS-NH_2-g-SWCNTs (1.0 wt%) shows about 26% higher strength than the reference sample, due to the more effective reinforcement effect of the polymer-grafted SWCNTs combined with the slightly higher σ_y (~12%) of the aminated derivative as compared to that of the pure matrix (~64 MPa). It is worth mentioning that the improvements in E and σ_y attained in the nanocomposites reinforced with PPS-NH_2-g-SWCNTs are larger than those reported by Yu et al. [17] for PPS/MWCNT composites, where the modulus and strength improved only marginally up to 1.0 wt% MWCNTs. This indicates the effectiveness of the grafting process used in this work to enhance the mechanical properties of PPS. Regarding the elongation at break (Fig. 5c), a strong dependence on the CNT concentration is found. ε_b of the matrix increases by about 14% at 0.1 wt% SWCNTs, albeit decreases at higher loadings. This drop in ductility is smaller for the composites incorporating PPS-NH_2-g-SWCNTs, where ε_b decreases only slightly (~13 and 3% at 1.0 and 0.5 wt% nanotube loading, respectively). However, for the reference composite it falls considerably (nearly 50%), ascribed to the presence of agglomerates that restrain the plastic deformation of the matrix.

The toughness of the nanocomposites, measured as the area under the stress–strain curves (Fig. 5d), is also strongly influenced by the filler content. Moderate increases (~21 and 14%) are found at 0.1 and 0.5 wt% SWCNTs anchored to PPS-NH_2, respectively, whereas at higher concentrations the toughness is approximately maintained. However, the direct addition of 1.0 wt% loading brings along a decrease in toughness of 33%. This behaviour can be explained considering that the agglomerates initiate the cracks and promote the formation of dimples, leading to a premature failure. The covalent attachment of PPS-NH_2 onto the SWCNT surfaces results in a significant increase in the toughness of these composites, probably due to the combination of several synergic effects: a more homogeneous nanotube dispersion that reduces the stress concentration sites, a stronger SWCNT-matrix interfacial adhesion that prevents the propagation of cracks, and the presence of PPS-NH_2, which exhibits higher toughness than neat PPS due to the increase in the degree of crosslinking of the polymer chains through hydrogen bonds and its lower crystallinity [19,36].

To further evaluate the toughness of the composites, Charpy notched impact strength measurements were carried out, and the experimental data are displayed in Table 1. Neat PPS exhibits low impact strength (~2 kJ m^{-2}), and it increases by about 32% with the incorporation of 0.1 wt% SWCNTs, consistent with the larger extent of plastic deformation of this sample, as revealed by tensile tests. The composite with 0.5 wt% SWCNT loading shows approximately 20% higher impact strength than the matrix, whilst that reinforced with 1.0 wt% content exhibits nearly the same value. Nevertheless, a drop of 30% is observed for the reference sample. These results follow similar trends to those discussed above for the areas under the tensile curves (Fig. 5d), and also correlate well with the analysis of the areas under dynamic mechanical peaks (Fig. 2). Any molecular process that promotes energy dissipation enhances the impact resistance of the polymer, as indicated by Kausch's statement [37]. The data obtained from the different techniques reveal that the incorporation of small amounts of PPS-NH_2-g-SWCNTs favours the energy dissipation, hence improves the impact resistance of the matrix.

The flexural properties of the nanocomposites were also investigated, and the results are collected in Table 1. The flexural modulus E_f of PPS increases by 14, 30 and 39% with the addition of 0.1, 0.5 and 1.0 wt% SWCNT loadings, respectively, mirroring the trend observed for the Young's moduli. Analogously, the enhancements in flexural strength σ_f are about 9, 20 and 24% for the above indicated nanotube contents. The comparison with the increments obtained for the reference composite (~19 and 10% in E_f and σ_f, respectively) corroborates that the grafting of the aminated derivative onto the SWCNTs improves considerably their reinforcing efficiency.

3.5. Tribological properties

Fig. 6a shows the evolution of the friction coefficient (μ) as a function of the sliding distance for neat PPS and the nanocomposites with different SWCNT content. As can be observed, μ of PPS increases considerably at the beginning of the tribological test,

Table 1
Mechanical parameters derived from the flexural and Charpy impact tests of PPS/PPS-NH_2-g-SWCNT nanocomposites: flexural modulus (E_f), flexural strength (σ_{fm}), impact force (F) and impact strength (E_{charpy}). For comparison, data of the reference composite with 1.0 wt% SWCNTs (designated by an asterisk) are also included.

SWCNT content (wt%)	Flexural tests		Charpy impact tests	
	E_f (GPa)	σ_{fm} (MPa)	F (N)	E_{charpy} (kJ m^{-2})
0	3.14 ± 0.13	112.1 ± 2	320 ± 20	1.94 ± 0.21
0.1	3.58 ± 0.10	122.8 ± 2	380 ± 30	2.56 ± 0.28
0.5	4.06 ± 0.15	134.5 ± 4	430 ± 50	2.33 ± 0.25
1.0	4.37 ± 0.19	139.6 ± 5	460 ± 40	1.89 ± 0.22
1.0*	3.73 ± 0.17	123.7 ± 5	390 ± 30	1.35 ± 0.19

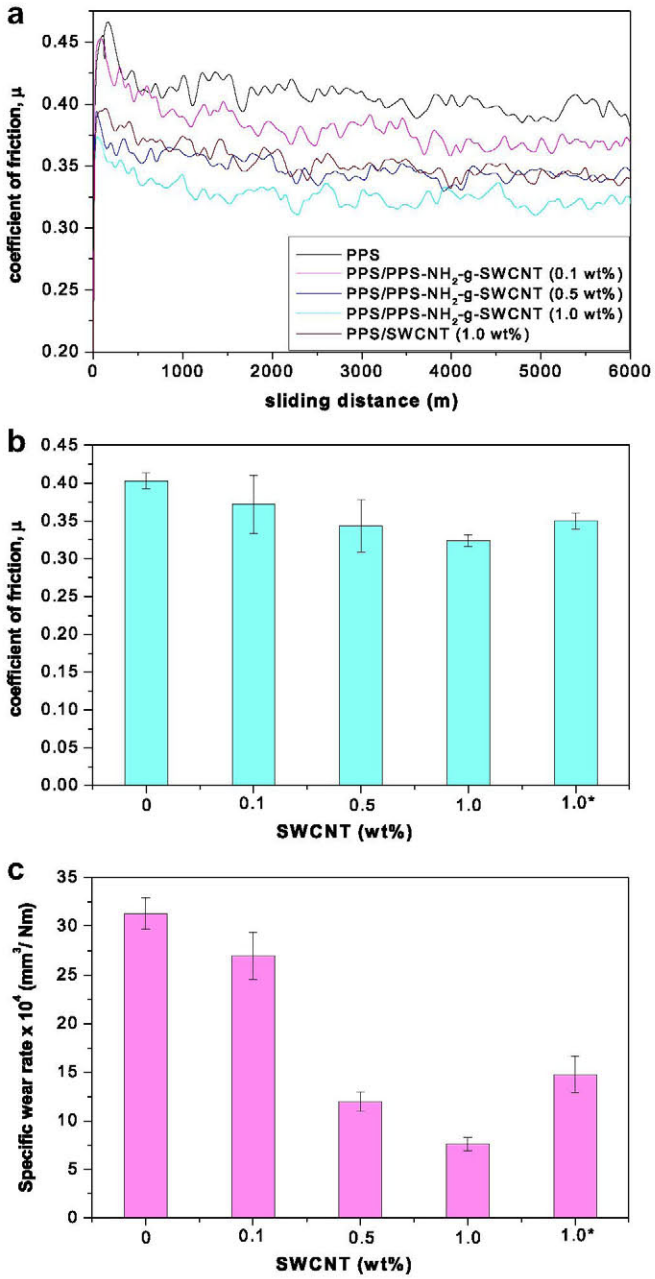

Fig. 6. Tribological properties of neat PPS and the nanocomposites: (a) Friction coefficient as a function of the sliding distance. (b) Mean friction coefficient and (c) specific wear rate as a function of SWCNT content.

ascribed to a progressive increase in temperature, which leads to a decrease in the elastic modulus, hence a deeper indentation of the steel asperities into the polymer and an increase in the real contact area between them. Consequently, the sliding between the steel counterpart and PPS surfaces requires more polymer deformation, resulting in higher μ. After a certain sliding distance, the friction force and the temperature reach a maximum; at this point, the shear strength of the softer material is lower, making the sliding between the polymer and the counterpart surfaces easier, thus the friction coefficient decreases, and then reaches a steady state trend [38]. Similar behaviour is found for nanocomposites with very low SWCNT loadings; however, for the samples with 1.0 wt% SWCNT content, this initial increase is less pronounced, and could be related to the higher thermal conductivity of the nanocomposite, which facilitates heat dissipation, leading to a smaller increase in temperature. Moreover, the presence of the nanofiller makes the nanocomposite surface harder, hence reduces the penetration of the counterpart into the matrix.

The mean friction coefficient as a function of the SWCNT loading is depicted in Fig. 6b. The addition of increasing contents of PPS-NH_2-g-SWCNTs leads to a gradual decrease in μ, the reduction being about 17% at 1.0 wt% loading. This behaviour can be attributed to several factors, including the improvement in mechanical properties (i.e. modulus, strength, hardness, etc.) and the increase in thermal conductivity that lowers the temperature in the sliding contact; these facts reduce the indentation of the counterpart into the matrix. Moreover, the polymer might have been removed from the composite surface during the initial stage of the test, hence the SWCNTs are more exposed to the sliding interface, and act as solid lubricants, thus facilitating the frictional sliding. The abovementioned synergic effects rise as the SWCNT content increases, thereby leading to a reduction in μ. In the case of the composite prepared by direct integration of 1.0 wt% SWCNTs, the decrease was only about 12% in comparison to the μ of neat PPS. The discrepancy can be explained considering that this nanocomposite exhibits less significant improvement in mechanical properties, as revealed by tensile and flexural tests. Moreover, the presence of small agglomerates probably results in less effective lubricant effect and lower thermal conductivity, hence higher temperature in the sliding contact as compared to the composites incorporating PPS-NH_2. Yu et al. [39] compared the friction coefficient of neat PPS and composites reinforced with dry lubricants like graphite, MoS_2 and PTFE, and found that PPS/graphite composite exhibited the lowest μ, ascribed to its improved mechanical properties. Similar behaviour is found in this work, where the lowest μ is observed for the nanocomposite with enhanced modulus and strength.

Regarding the wear rate (Fig. 6c), a strong decrease is found with the addition of the SWCNTs as compared to that of neat PPS; the nanocomposite with PPS-NH_2-g-SWCNTs (1.0 wt%) shows a reduction of about 75%. This enhancement in wear resistance is ascribed to the high strength of the CNTs, which restrain the scuffing and adhesion of the matrix in sliding, providing a much better resistance than the neat PPS, combined with the abovementioned lubricant effect and the increased thermal conductivity of the composite. Moreover, the nanotubes act as a barrier and prevent large-scale fragmentation of the polymer. This is in agreement with the behaviour reported by Co et al. [16] for CNF-reinforced PPS composites, where the wear rate decreased by a factor of 3 for 1.0 vol% CNFs. As expected, the improvement in wear resistance is less pronounced for the reference composite as compared to that incorporating the aminated derivative with the same SWCNT content, related again to its lower load bearing capacity. Furthermore, surface functionalization of the CNTs enhances the wettability and the CNT-matrix interfacial adhesion, another factor that is known to improve the wear resistance of composites [40]. Therefore, the SWCNTs grafted with a polymer derivative can be considered as promising tribological additives for thermoplastic polymers.

3.6. Contact angle measurements

Taking into account that the surface energy (σ) is a key parameter determining the tribological properties of the material, it is interesting to analyse the influence of these SWCNTs on σ of PPS matrix. The total surface energy and its polar and dispersion components for PPS and the nanocomposites were calculated using contact angle measurements according to Eq. (1), and the results are plotted in Fig. 7. The changes in σ indicate the existence of

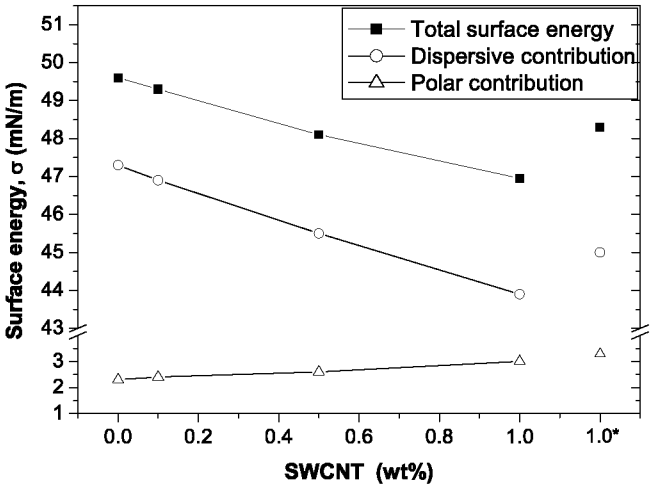

Fig. 7. Total surface energy σ and its polar (σ_p) and dispersion (σ_d) components for neat PPS and the nanocomposites, obtained through contact angle measurements.

strong interactions between the matrix and the acid-treated SWCNTs. The total surface energy of PPS is about 50 mN m^{-1}, and decreases slightly and progressively with increasing SWCNT content, the reduction being around 6% for the composite with 1.0 wt% loading of grafted fillers. Similar trend is observed for the dispersive contribution, whereas the polar component increases moderately, due to the unreacted NH_2 groups of the aminated derivative and the carboxylic groups of the SWCNT sidewalls, which increase the hydrophilicity of the composite surface. The change in the polar component is higher for the sample prepared by direct integration of the SWCNTs, since exhibits larger number of free COOH groups. However, the decrease in total surface energy is smaller, which is consistent with the less pronounced decrease in wear rate and friction coefficient observed for this reference composite. Therefore, the results indicate the existence of a correlation between the surface energy and the tribological properties of these nanocomposites.

4. Conclusions

PPS based nanocomposites were fabricated via melt-blending by the addition of an aminated derivative covalently grafted onto the surface of acid-treated SWCNTs. Their surface energy, viscoelasticity, electrical, mechanical and tribological properties have been evaluated as a function of the nanotube loading, and compared to those of a reference composite reinforced directly with 1.0 wt% SWCNTs. SEM micrographs revealed that the polymer grafting enhanced the nanotube dispersion within the matrix. DMA experiments demonstrated noticeable improvements in the storage and loss moduli as well as in the glass transition temperature with increasing SWCNT content. At high temperature, the moduli vs. frequency curves tended to a plateau in the low-frequency regime, indicating a transition from liquid-like to solid-like viscoelastic behaviour. The electrical conductivity of the nanocomposites increased sharply around 0.25 wt% SWCNT loading, reflecting percolation behaviour. Both electrical and rheological percolation thresholds took place at similar SWCNT concentrations. Tensile and flexural properties as well as impact strength improved significantly in comparison with those of the reference composite, since the covalent interactions and hydrogen bonds enhanced the load transfer efficiency. A good correlation was found between the toughness of the nanocomposites measured as the area under the tensile curves, the impact strength obtained from Charpy impact tests and the area under dynamic mechanical peaks. The surface energy, friction coefficient and wear rate of PPS decreased with the incorporation of PPS-NH_2-g-SWCNTs; the enhancement in tribological properties is ascribed to the lubricant effect of the SWCNTs and the higher thermal conductivity of the composites. Taking into account that PPS is a high-cost high-performance polymer, the elevated price of the SWCNTs and the feasibility as well as relatively low cost of the grafting process used in this work, it can be concluded that the improvements in properties attained by the addition of PPS-NH_2-g-SWCNT to the polymer matrix are cost-effective. The results indicate that this is a promising approach to improve the overall performance of thermoplastic polymers such as PPS for structural applications.

Acknowledgements

Financial support from the Ministerio de Ciencia e Innovación (MICINN, Project MAT2010-21070-C02-01) is gratefully acknowledged. Dr. A. Diez would like to thank to the MICINN for Juan de la Cierva postdoctoral contract. Dr. M. Naffakh would like to acknowledge the Consejo Superior de Investigaciones Cientificas (CSIC) for a Postdoctoral Contract through Intramural Research Project No. 201160E003) and the Ministerio de Economía y Competitividad (MINECO) for a 'Ramón y Cajal' Research Fellowship.

Appendix A. Supplementary material

Supplementary data related to this article can be found online at doi:10.1016/j.matchemphys.2012.04.057.

References

[1] M. Moniruzzaman, K.I. Winey, Macromolecules 39 (2006) 5194–5205.
[2] E.T. Thostenson, Z. Ren, T.-W. Chou, Compos. Sci. Technol. 61 (2001) 1899–1912.
[3] Z. Spitalsky, D. Tasis, K. Papagelis, C. Galiotis, Prog. Polym. Sci. 35 (2010) 357–401.
[4] S. Yesil, G. Bayram, Polym. Eng. Sci. 51 (2011) 1286–1300.
[5] J. Chen, M.A. Hamon, H. Hu, Y. Chen, A.M. Rao, P.C. Eklund, R.C. Haddon, Science 282 (1998) 95–98.
[6] D.E. Hill, Y. Lin, A.M. Rao, L.F. Allard, Y.-P. Sun, Macromolecules 35 (2002) 9466–9471.
[7] Y. Lin, B. Zhou, K.A.S. Fernando, P. Liu, L.F. Allard, Y.-P. Sun, Macromolecules 36 (2003) 7199–7204.
[8] B. Fragneaud, K. Masenelli-Varlot, A. Gonzalez-Montiel, M. Terrones, J.Y. Cavaillé, Compos. Sci. Technol. 68 (2008) 3265–3271.
[9] B.-X. Yang, J.-H. Shi, K.P. Pramoda, S.H. Goh, Compos. Sci. Technol. 68 (2008) 2490–2497.
[10] D.G. Brady, J. Appl. Polym. Sci. Appl. Polym. Symp. 36 (1981) 231–239.
[11] H.W. Hill, D.G. Brady, Polym. Eng. Sci. 16 (1976) 831–835.
[12] H. Wayne, H.W. Hill, D.G. Brady, Encyclopedia of Polymer Science and Engineering, vol. 11, Willey, New York, 1988, p. 531.
[13] V.L. Shangankuli, J.P. Jog, V.M. Nadkani, J. Appl. Polym. Sci. 36 (1988) 335–351.
[14] M. Naffakh, C. Marco, M.A. Gómez, I. Gómez-Herrero, I. Jiménez, J. Phys. Chem. B 113 (2009) 10104–10111.
[15] M. Naffakh, C. Marco, M.A. Gómez, I. Jiménez, J. Phys. Chem. B 112 (2008) 14819–14828.
[16] M.H. Co, S. Bahadur, Tribol. Lett. 25 (2007) 237–245.
[17] S. Yu, W.M. Wong, S. Hu, Y.K. Juay, J. Appl. Polym. Sci. 113 (2009) 3477–3483.
[18] J. Yang, T. Xu, A. Lu, Q. Zhang, H. Tan, Q. Fu, Compos. Sci. Technol. 69 (2009) 147–153.
[19] H.N. Beck, J. Appl. Polym. Sci. 45 (1992) 1361–1366.
[20] A.M. Diez-Pascual, M. Naffakh, Mater. Chem. Phys. 131 (2012) 605–614.
[21] D.K. Owens, R.C. Wendt, J. Appl. Polym. Sci. 13 (1969) 1741–1747.
[22] S.J. Oh, H.J. Lee, D.K. Keum, S.W. Lee, D.H. Wang, S.Y. Park, L.-S. Tan, J.-B. Baek, Polymer 47 (2006) 1132–1140.
[23] A.M. Diez-Pascual, G. Martinez, M.T. Martinez, M.A. Gomez, J. Mater. Chem. 20 (2010) 8247–8256.
[24] M. Wang, K.P. Pramoda, S.H. Goh, Polymer 46 (2005) 11510–11516.
[25] S.H. Jafari, A.K. Gupta, J. Appl. Polym. Sci. 78 (2000) 962–971.
[26] A.M. Diez-Pascual, M. Naffakh, M.A. Gómez, C. Marco, G. Ellis, M.T. Martínez, A. Ansón, J.M. González-Domínguez, Y. Martínez-Rubi, B. Simard, Carbon 47 (2009) 3079–3090.
[27] J.D. Ferry, Viscoelastic Properties of Polymers, third ed. John Wiley & Sons, New York, 1980.

[28] F. Du, R.C. Scogna, W. Zhou, S. Brand, J.E. Fischer, K.I. Winey, Macromolecules 37 (2004) 9048–9055.
[29] P. Pötschke, M. Abdel-Goad, I. Alig, S. Dudkin, D. Lellinger, Polymer 45 (2004) 8863–8870.
[30] Y.F. Zhao, M. Xiao, S.J. Wang, X.C. Ge, Y.Z. Meng, Compos. Sci. Technol. 67 (2007) 2528–2534.
[31] J.Z. Kovacs, B.S. Velagala, K. Schulte, W. Bauhofer, Compos. Sci. Technol. 67 (2007) 922–928.
[32] A. Noll, T. Burkhart, Compos. Sci. Technol. 71 (2011) 499–505.
[33] X. Feng, G. Liao, Q. He, X. Jian, J. Du, Polym. Compos. 30 (2009) 365–373.
[34] A.M. Díez-Pascual, M. Naffakh, J.M. González-Domínguez, A. Ansón, M.T. Martínez, Y. Martínez-Rubi, B. Simard, M.A. Gómez, Carbon 48 (2010) 3500–3511.
[35] E.W. Wong, P.E. Sheehan, C.M. Lieber, Science 277 (1997) 1971–1975.
[36] D. Lu, Y.-W. Mai, R.K.Y. Li, L. Ye, Macromol. Mater. Eng. 288 (2003) 693–698.
[37] C. Grein, C.J.G. Plummer, Y. Germain, H.H. Kausch, P. Béguelin, Polym. Eng. Sci. 43 (2003) 223–233.
[38] N.E. Bekhet, Wear 236 (1999) 55–61.
[39] L. Yu, S. Yang, W. Liu, Q. Xue, Polym. Eng. Sci. 40 (2000) 1825–1832.
[40] J. Li, Surf. Interf. Analys. 41 (2009) 759–763.